Design, Synthesis, Crystal Structure, and Host−Guest Properties of Polymethylene-Bridged Cystine-Based Cyclobisamides: A Facile Entry into Hydrogen-Bonded Peptide Nanotubes†

Darshan Ranganathan,*,‡ V. Haridas,‡ C. Sivakama Sundari,§ D. Balasubramanian,⊥ K. P. Madhusudanan,∥ Raja Roy,∥ and Isabella L. Karle*,○

Discovery Laboratory, Indian Institute of Chemical Technology, Hyderabad-500 007, India, Hyderabad Eye Research Foundation, L.V. Prasad Eye Institute, Hyderabad-500 034, India, Centre for Cellular and Molecular Biology, Hyderabad-500 007, India, Central Drug Research Institute, Lucknow-226 001, India, and Laboratory for the Structure of Matter, Naval Research Laboratory, Washington, D.C. 20375-5341

Received August 31, 1999

A general design strategy for the synthesis of cystine-based peptide nanotubes is described. The design essentially involves closing of the polymethylene chains with cystine diOMe. The cystine-based nanotubes are constructed by the self-assembly of a simple cyclobisamide building block, a key structural feature of which is the presence of two amide groups at almost opposite poles of the ring. A large variety of cyclobisamides with the general structure cyclo(−CO−$(CH_2)_n$−CO−Cyst−) have been prepared by a single-step procedure involving the condensation of 1,ω-alkane dicarbonyl dichloride [$(CH_2)_n(COCl)_2$, n = 2, 3, ..., 10, 20] with cystine diOMe providing macrocyclic bisamides with ring size varying from 14 to 30 members. Single-crystal X-ray studies with four members (n = 4, 6, 8, and 10, respectively) have shown that the polymethylene-bridged cystine-based cyclobisamides possess the intrinsic property of self-assembling into highly ordered parallel arrays of solid-state nanotubes. The hydrogen-bonded cystine tubes are hollow and open ended and extend to infinity. The interior of the tubes is totally hydrophobic. As a result, the polymethylene-bridged peptide tubes (a) are able to enhance the solubility of highly lipophilic compounds in water, as demonstrated here, with pyrene and perylene polycyclic arenes, (b) are able to bind to fluorescent probe dyes such as Nile Red, and (c) can even induce an ordered secondary structure in linear peptides as shown here with the 26-residue bee-venom peptide melittin, in the 30-membered cystine tubule. Crystallographic parameters are ($C_{14}H_{22}N_2O_6S_2$, $P2_12_12$) a = 16.489(1) Å, b = 23.049(1) Å, c = 4.864(1) Å; ($C_{16}H_{26}N_2O_6S_2$, $P2_12_12$) a = 19.171(2) Å, b = 21.116(2) Å, c = 5.0045(4) Å; ($C_{18}H_{30}N_2O_6S_2$, $P2_12_12_1$) a = 5.022(1) Å, b = 17.725(3) Å, c = 25.596(2) Å; and ($C_{20}H_{34}N_2O_6S_2$, $C2$) a = 40.698(15) Å, b = 5.083(3) Å, c = 12.105(5) Å, β = 99.66(3)°.

Introduction

Tubular structures have gained unprecedented importance in recent years because of their demonstrated potential in chemical, biological, and material science applications. Recent literature abounds with reports of the creation of nanotubes from inorganic and organic substances such as graphite,[1] boron nitride,[2] tungsten disulfide,[3] zeolites,[4] lipids,[5] carbohydrates,[6] and peptide-based nanotubes.[7]

Tubular structures constructed from chiral amino acids are particularly useful as mimics for biological transport systems or for encapsulating guest molecules, with potential applications in drug delivery and catalysis, or they can be exploited as constrained environments to design nanostructured biomaterials. A strategy that has emerged as the most popular approach for creating hydrogen-bonded, open-ended, hollow peptide tubes is through the stacking of cyclopeptide rings.[7−11]

Several designs of cyclopeptides, for example, cyclopeptides composed of an equal number of α- and β-amino acids,[9] or all β-amino acids,[10,11] or even numbers of alternating D- and L-amino acids[7,8] have been reported and demonstrated to self-assemble into hollow, open-ended tubular structures through backbone−backbone NH···O═C hydrogen bonding.

On the basis of simple model building, we envisaged that cystine-based cyclobisamides wherein the amide groups are positioned at two opposite poles of the ring can act as excellent candidates for creating tubular

* To whom correspondence should be addressed.

† Dedicated to Professor S. Ranganathan on the occasion of his 65th birthday.

‡ Indian Institute of Chemical Technology. Fax: 91-40-7173757.
§ Centre for Cellular and Molecular Biology.
⊥ L.V. Prasad Eye Institute.
∥ Central Drug Research Institute.
○ Naval Research Laboratory. Fax: 202-767-6874.

(1) (a) Lijima, S. *Nature* **1991**, *354*, 56. (b) Ajayan, P. M.; Ebbeson, T. W. *Rep. Prog. Phys.* **1997**, *60*, 1025. (c) Wong, S. S.; Joselevich, E.; Woolley, A. T.; Cheung, C. Li.; Lieber, C. M. *Nature* **1998**, *394*, 52.

(2) Chopra, N. G.; Luyken, R. J.; Cherry, K.; Crespi, V. H.; Cohen, M. L.; Louie, S. G.; Zettl, A. *Science* **1995**, *269*, 966.

(3) Tenne, F.; Margulis, L.; Genut, M.; Hodes, G. *Nature* **1992**, *360*, 444.

(4) (a) Meier, W. M.; Olson, D. H. *Atlas of Zeolite Structure Types*; Butterworths: London, 1988. (b) Dessau, R. M.; Schlenker, J. L.; Higgins, J. B. *Zeolites* **1990**, *10*, 522. (c) Munoz, T.; Balkus, K. J., Jr. *J. Am. Chem. Soc.* **1999**, *121*, 139.

(5) Lee, Y.-S.; Yang, J.-Z.; Sisson, T. M.; Frankel, D. A.; Gleeeson, J. T.; Aksay, M.; Kellar, S. L.; Gruner, S. M.; O′Brien, D. F. *J. Am. Chem. Soc.* **1995**, *117*, 5573.

(6) (a) Harada, A.; Kamachi, J. Li. M. *Nature* **1993**, *364*, 516. (b) Gattuso, G.; Menzer, S.; Nepogodiev, S. A.; Stoddart, J. F.; Williams, D. J. *Angew. Chem., Int. Ed. Engl.* **1997**, *36*, 1451. (c) Benner, K.; Klufers, P.; Schumacher, J. *Angew. Chem., Int. Ed. Engl.* **1997**, *36*, 743.

(7) De Santis, P.; Morosetti, S.; Rizzo, R. *Macromolecules* **1974**, *7*, 52.

10.1021/jo991378m CCC: $18.00
Published on Web 11/12/1999

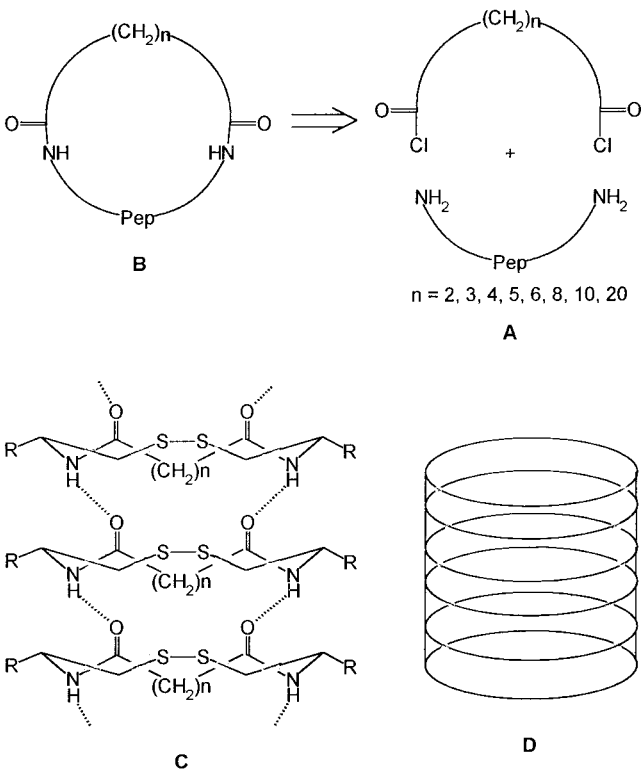

Figure 1. Design strategy for crafting cystine-based cyclobisamide tubes. The simple cyclobisamides (B) with amide groups positioned at two opposite poles of the ring constructed in a single step from 1,ω-alkane dicarbonyl dichloride and cystine diOMe (A) can stack atop one another through backbone−backbone (NH···O═C) hydrogen bonding (C), extending into hydrogen-bonded open-ended peptide nanotubes (D).

structures by stacking on top of each other through contiguous amide−amide hydrogen bonding (Figure 1).

We provide herein the first illustration of this concept, report on the construction of polymethylene-bridged cystine-based cyclobisamides—a new class of macrocyclic peptides with the general structure cyclo(−CO−$(CH_2)_n$−CO−Cyst−), and demonstrate the intrinsic property of these macrocycles to assemble in vertical stacks of hydrogen-bonded, open-ended tubular structures.

The interior of the tubes is hydrophobic with a polarity comparable to that of a nonpolar organic solvent. As a result, these cystine tubules possess the power to solubilize highly lipophilic compounds and to bind to fluorescent probe dyes. The wider tubules can even induce an ordered conformation in peptides, as shown here with 26-residue bee-venom peptide melittin adopting a largely α-helical structure in the 30-membered cystine tubule.

Results and Discussion

Synthesis and Characterization. The cystine-based cyclobisamides with the general structure cyclo (−CO−$(CH_2)_n$−CO−Cyst−) (Cyst = NH−CH(CO_2Me)CH_2−S−S−CH_2−CH(CO_2Me)−NH, n = 2−6, 8, 10, 20) were constructed in a single step by the reaction of freshly prepared 1,ω-alkane dicarbonyl dichloride [$(CH_2)_n(COCl)_2$, **1**] with simple L-cystine dimethyl ester (**2**) under high-dilution conditions in dry CH_2Cl_2 in the presence of triethylamine. As shown in Chart 1, the desired [1 + 1] cyclization product was invariably mixed with cyclic oligomers arising from higher order cyclization reaction except in the case of dodecyl (n = 10) and docosyl (n = 20) dicarbonyl dichlorides wherein the [1 + 1] cyclization product was the only isolated reaction product. The modest yield of ∼20−50% of the total cyclic product in the cyclization reaction is attributed to the formation of linear polymers in a parallel side reaction. While [1 + 1] cyclization product was obtained in every case, and [2 + 2] in most cases (n = 2 ... 8), the products of higher order cyclizations of [3 + 3] and [4 + 4] were seen only with n = 3 ... 6. Interestingly, glutaryl chloride (n = 3) was the only case where [5 + 5] and [6 + 6] cyclization products were isolated (Figure 2). It was however gratifying to note that the yield of [1 + 1] cyclization product increases with an increase in the value of n, the optimum being ∼30% with n = 6, 8, or 10. Chart 1 presents the breakup of yields obtained with various dicarbonyl dichlorides. From the yield distribution it appears that ring size may be the main controlling factor in the cyclization reaction, with a 16−20-membered ring being the optimum size for maximum yield. Although macrocycles with a ring size as large as 78-membered ([6 + 6] cyclization product with n = 3) have been obtained, their yields are abysmally poor and may be formed as a statistical chance.

The design is flexible with respect to the ring size, and the diameter can easily be adjusted by choosing dicarbonyl dichlorides of appropriate length as illustrated here with the preparation of cystine-based cyclobisamides ranging in ring size from 12- to 30-membered. The presence of COOH groups (as protected esters) on the exterior of the ring provides attractive handles for anchoring a variety of ligands that may lead to cyclobisamides with modified surface properties. The [1 + 1] cyclobisamides could easily be separated from cyclic oligomers by careful chromatography on silica gel columns using a gradient elution with the chloroform/methanol solvent system. The cyclooligomers were fully characterized by spectral and analytical data. The high symmetry in the products of [1 + 1] ... [6 + 6] cyclization was indicated by the presence of just a single set of resonances for the cystine and polymethylene units in their ^{1}H NMR spectra. Figure 3 presents a comparison of the ^{1}H NMR spectra of the cyclic monomer to pentamer (a−e) in the glutaryl (n = 3) series. Interestingly, the cystine resonances (Cβ protons in particular) in the smallest macrocycle [(Glut-Cyst)$_n$, n = 1] move

(8) (a) Ghadiri, M. R.; Granja, J. R.; Milligan, R. A.; McRee, D. E.; Khazanovich, N. *Nature* **1993**, *366*, 324. (b) Ghadiri, M. R.; Granja, J. R.; Buehler, L. K. *Nature* **1994**, *369*, 301. (c) Granja, J. R.; Ghadiri, M. R. *J. Am. Chem. Soc.* **1994**, *116*, 10785. (d) Khazanovich, N.; Granja, J. R.; McRee, D. E.; Milligan, R. A.; Ghadiri, M. R. *J. Am. Chem. Soc.* **1994**, *116*, 6011. (e) Ghadiri, M. R. *Adv. Mater.* **1995**, *7*, 675. (f) Ghadiri, M. R.; Kobyashi, K.; Granja, J. R.; Chadha, R. K.; McRee, D. R. *Angew. Chem., Int. Ed. Engl.* **1995**, *34*, 93. (g) Kobyashi, K.; Granja, J. R.; Ghadiri, M. R. *Angew. Chem., Int. Ed. Engl.* **1995**, *34*, 95. (h) Clark, T. D.; Ghadiri, M. R. *J. Am. Chem. Soc.* **1995**, *117*, 12364. (i) Engels, M.; Bashford, D.; Ghadiri, M. R. *J. Am. Chem. Soc.* **1995**, *117*, 9151. (j) Hartgerink, J. D.; Granja, J. R.; Milligan, R. A.; Ghadiri, M. R. *J. Am. Chem. Soc.* **1996**, *118*, 43. (k) Motesharei, K.; Ghadiri, M. R. *J. Am. Chem. Soc.* **1997**, *119*, 11306. (l) Kim, H. S.; Hartgerink, J. D.; Ghadiri, M. R. *J. Am. Chem. Soc.* **1998**, *120*, 4417. (m) Hartgerink, J. D.; Clark, T. D.; Ghadiri, M. R. *Chem. Eur. J.* **1998**, *4*, 1367.

(9) (a) Hassall, C. H. In *Proceedings of the Third American Peptide Symposium*; Meinhoffer, J., Ed.; Ann Arbor Science: Ann Arbor, MI, 1972; pp 153−157. (b) Karle, I. L.; Handa, B. K.; Hassall, C. H. *Acta Crystallogr.* **1975**, *B31*, 555.

(10) Seebach, D.; Matthews, J. L.; Meden, A.; Wessels, T.; Baerlocher, C.; McCusker, J. B. *Helv. Chim. Acta* **1997**, *80*, 173.

(11) Clark, T. D.; Buchler, L. K.; Ghadiri, M. R. *J. Am. Chem. Soc.* **1998**, *120*, 651.

Chart 1. Product Distribution of Cyclic Oligomers in the Synthesis of Polymethylene-Bridged Cystine-Based Cyclobisamides

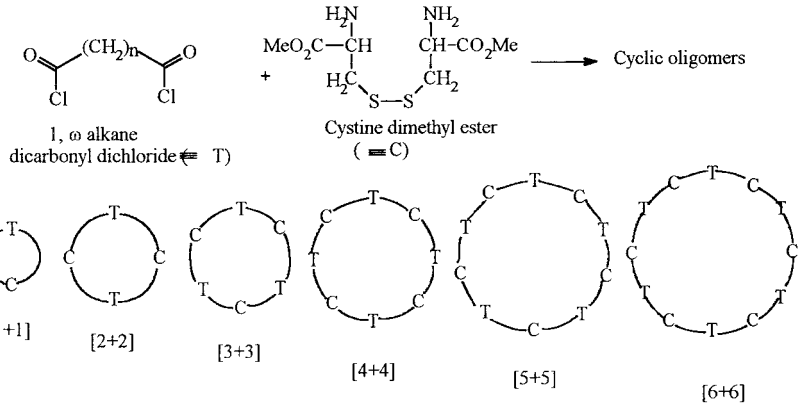

n	Mode of cyclization Yield % (ring size)					
	1+1	2+2	3+3	4+4	5+5	6+6
2	11.8 (12)	9.10 (24)	-	-	-	-
3	9.3 (13)	20.3 (26)	5.4 (39)	1.5 (52)	0.3 (65)	0.2 (78)
4	20.46 (14)	1.2 (28)	1.0 (42)	-	-	-
5	10.55 (15)	3.0 (30)	2.0 (45)	1.15 (60)	-	-
6	30.0 (16)	16.0 (32)	5.0 (48)	-	-	-
8	31.0 (18)	15.0 (36)	-	-	-	-
10	29.0 (20)	-	-	-	-	-
20	20.0 (30)	-	-	-	-	-

slightly upfield compared to those in the higher (Glut-Cyst)$_n$ (n = 2 ... 6) members. This may be attributed to the increased conformational constraints in the 13-membered Glut-Cyst macrocycle. The cyclic oligomeric nature of cyclization products was confirmed by FAB MS spectra. Figure 4 shows a comparison of FAB MS spectra of the cyclic monomer to hexamer (a−f) in the glutaryl (n = 3) series. No significant features were observed in the ROESY (rotating frame nuclear overhauser effect spectroscopy) NMR spectra of any of the macrocyclic bisamides except for some cross-peaks between the cystine NH's and the −CH_2's of the alkane unit in some higher cyclic oligomers, indicating trans orientation of the amide groups. In the ^{1}H NMR (DMSO-d_6), there was no indication of any intramolecular hydrogen bonding in any of the cyclobisamides or polyamides as shown by high-temperature coefficient values (−7 to −8 ppb/K) in variable-temperature (VT) studies. However, because of the poor solubility of cyclic oligomeric amides in common NMR solvents, concentration-dependent studies could not be carried out.

The formation of cyclic oligomers containing two, three, four, five, and six cyclic repeats of CO−$(CH_2)_n$−CO−Cyst units was rationalized on the basis of further cyclooligomerization of the initially formed linear ClOC−$(CH_2)_n$−CO−Cyst intermediate. This notion was supported by the isolation of small amounts of (∼5−10%) of the linear polymer of the CO$(CH_2)_n$CO−Cyst unit in each case.

Single-Crystal X-ray Studies. Poor solubility of macrocyclic bisamides in common organic solvents posed difficulty in crystallization. After extensive trials, suitable crystals for X-ray diffraction studies could be obtained for four cyclic bisamides [cyclo(−CO−$(CH_2)_4$−CO−Cyst−) (**3**), cyclo(−CO−$(CH_2)_6$−CO−Cyst−) (**4**), cyclo(−CO−$(CH_2)_8$−CO−Cyst−) (**5**), and cyclo(−CO−$(CH_2)_{10}$−CO−Cyst−) (**6**) with 14-, 16-, 18-, and 20-membered ring sizes, respectively] from a mixture of dimethyl sulfoxide and 1-octanol. Interestingly, the crystals appeared (gradually over a period of ∼5−6 months) at the interface of the solvent mixture, and only the cyclobisamides containing an even number of methylene units formed crystals. As represented in Figure 1C, the tubes with an odd number of methylene groups would have their amide carbonyls in 0° (compared to 180° for an even-carbon chain) orientation from one another, resulting in a very high dipole moment that may not favor crystal formation. The fine needles were carefully separated and examined by X-ray diffraction.

Crystal structures of cyclobisamides **3**, **4**, **5**, and **6** (with n = 4, 6, 8, and 10, respectively) revealed some common features. Thus, regardless of the ring size (14−20), all macrocycles adopted a crown-shaped architecture, with carbomethoxy groups extending outward and no internal hydrogen bonds. The amide groups are in a plane perpendicular to that of the ring. In this conformation, the rings are aligned parallel and stack on top of one

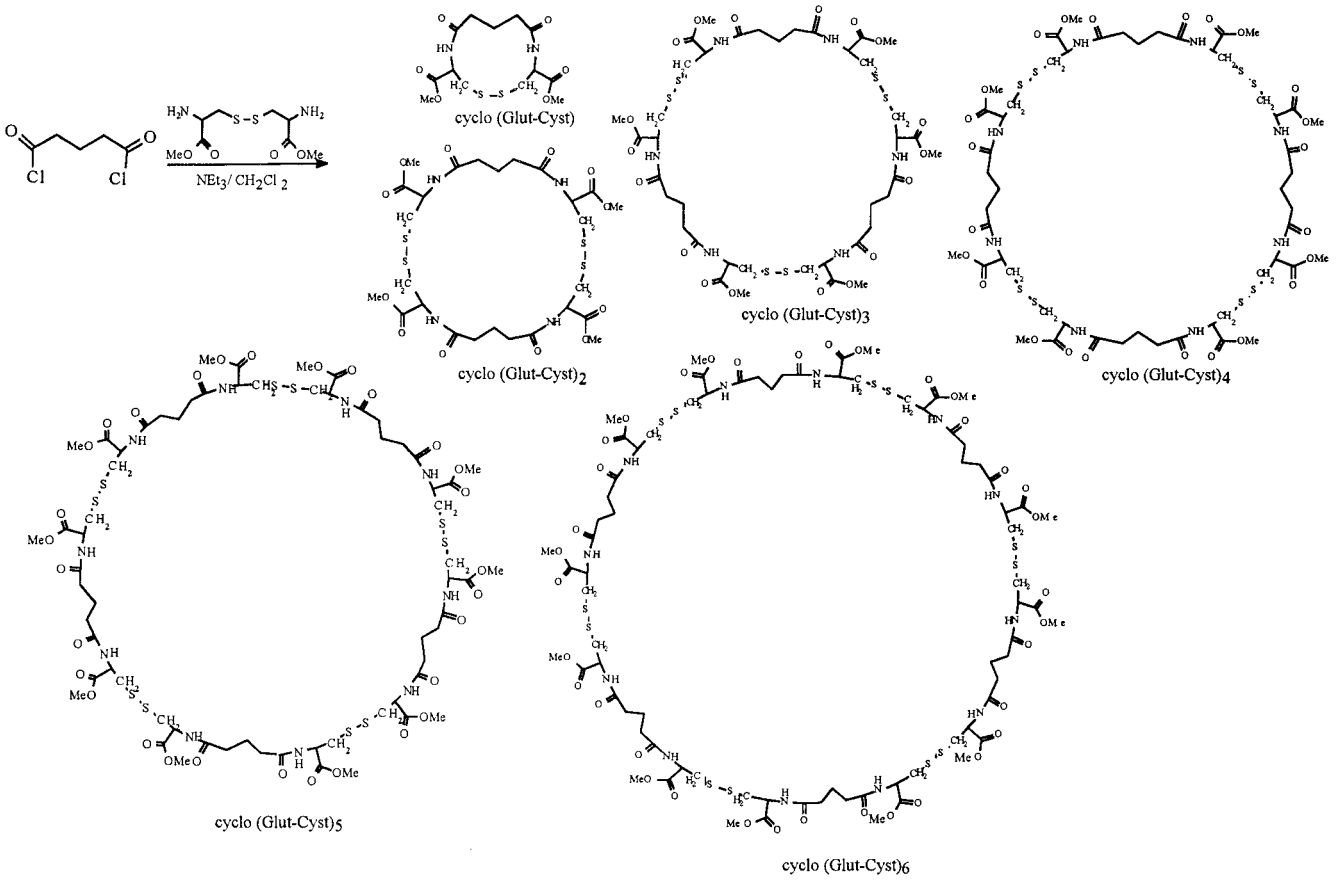

Figure 2. Cyclic oligomers of Glut−Cyst [Glut = $(CH_2)_3(CO)_2$; Cyst = $(-NH-CH(CO_2Me)-CH_2-S-)_2$]. The ring size varies from 13- to 78-membered from a cyclic monomer to a cyclic hexamer.

Table 1. Inter-Ring Distances and the Hydrogen Bond Parameters in the Nanotube Assembly of Cyclobisamides 3-6

cyclobisamide	inter-ring distance (Å)	hydrogen bond	N···O (Å)	H···O (Å)	N···OC angle (deg)
3	4.86	N1H···O0	3.002	2.13	167
		N2H···O02	2.948	2.06	166
4	5.00	N1H···O0	2.833	1.99	168
		N2H···O02	3.035	2.15	174
5	5.02	N1H···O0	2.932	2.05	177
		N2H···O02	2.899	2.02	173
6	5.08	N1H···O0	2.970	2.08	173
		N2H···O02	2.995	2.12	172

another through contiguous intersubunit amide−amide hydrogen bonding, forming extended tubular structures. The tubes are hollow and open ended and extend to infinity. In the pack, the tubes are held together only by van der Waals forces. The cavity size of the tubes varied between ∼5 Å (**3**) to ∼10 Å (**6**). Figures 5−8 (parts a−d) show, respectively, the molecular formula, crystal structure, vertical stacking of rings, and packing of nanotubes in the crystal of cyclobisamides **3**, **4**, **5**, and **6**.

The inter-ring distances and the hydrogen bond parameters in the nanotube assembly of cyclobisamides **3**−**6** are listed in Table 1. Some important angles and torsional angles are presented in Table 2.

The totally hydrophobic interior of the nanotubes (lined with polymethylenes) creates a nonpolar microenvironment that can be exploited for selective encapsulation of lipophilic substances.

Table 2. Some Important Bond Angles and Torsional Angles in Cyclobisamides 3−6 (deg)

	3	**4**	**5**	**6**
S2−S1−C1b	105	103	105	103
S1−S2−C2b	101	104	102	103
S1−C1b−C1a	114	112	117	116
S2−C2b−C2a	111	115	114	114
C1b−S1−S2−C2b	−90	97	−95	−87
C1a−C1b−S1−S2	−93	101	−63	−66
C2a−C2b−S2−S1	176	−53	−64	−70
C0′−N1−C1a−C1′	−153	−136	−110	−78
N1−C1a−C1′−O1m	−166	+61	−37	−31
C02′−N2−C2a−C2′	−140	−75	−101	−88
N2−C2a−C2′−O2m	+179	+157	+172	+128
N1−C0′−C1x−C2x	+86	+125	+130	+112
N2−C02′−Cpx−Cqx[a]	+82	+141	+123	+112

[a] Where p is the last C atom and q is the penultimate C atom in the $-(CH_2)_n-$ chain.

Inclusion Experiments and Host−Guest Properties. The interior of the polymethylene-bridged cystine tubes behaves like an apolar organic solvent and can enhance the solubility of highly lipophilic substances in water by selective host−guest complexation. This was demonstrated with extremely insoluble aromatic polycyclics, namely, pyrene and perylene. Figure 9a shows that while pyrene (with size ∼9.2 Å)[12] is unable to interact

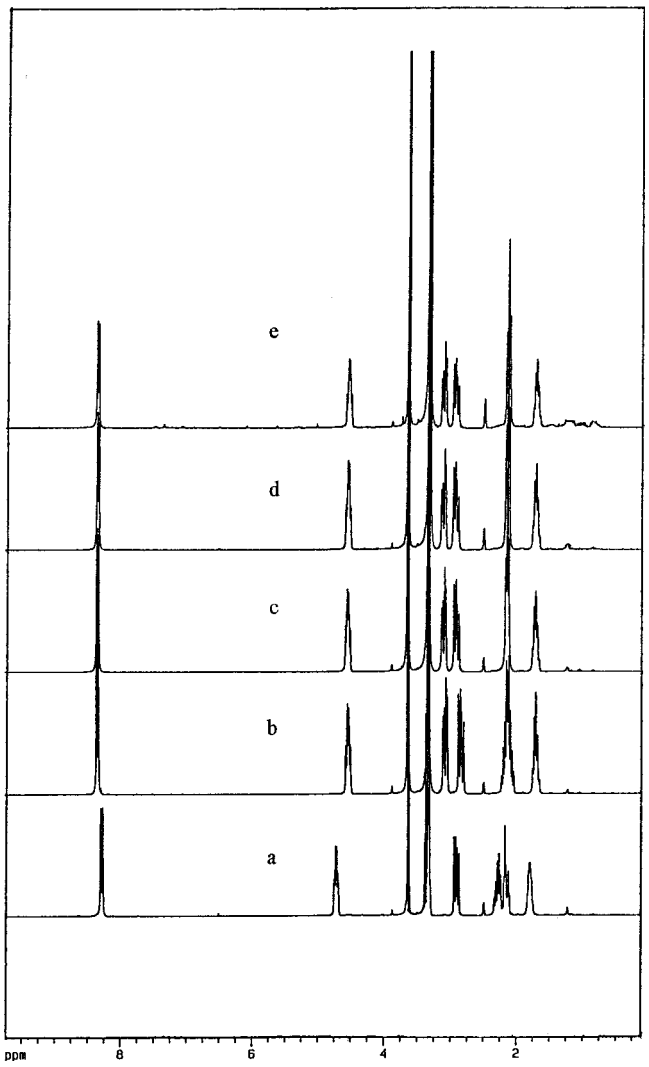

Figure 3. Comparison of ^{1}H NMR (300 MHz, DMSO-d_6) spectra of (a) cyclo(Glut−Cyst), (b) cyclo(Glut−Cyst)$_2$, (c) cyclo(Glut−Cyst)$_3$, (d) cyclo(Glut−Cyst)$_4$, and (e) cyclo(Glut−Cyst)$_5$.

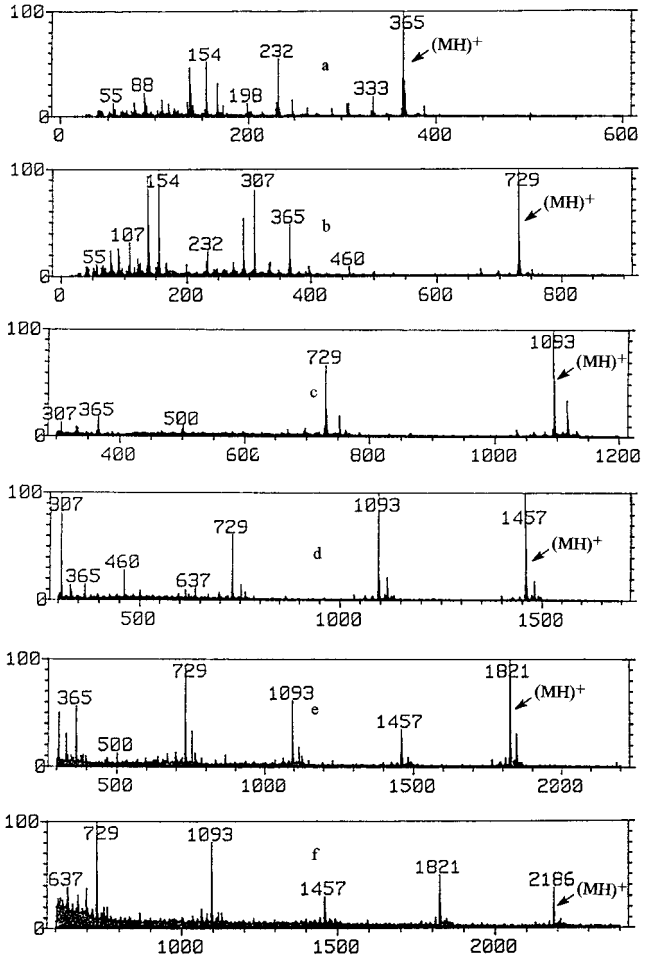

Figure 4. Comparison of FAB MS spectra of (a) cyclo(Glut−Cyst), (b) cyclo(Glut−Cyst)$_2$, (c) cyclo(Glut−Cyst)$_3$, (d) cyclo(Glut−Cyst)$_4$, (e) cyclo(Glut−Cyst)$_5$, and (f) cyclo(Glut−Cyst)$_6$.

with the cyclobisamide tube **5** (internal diameter ~5 Å), and can barely manage to do so with the larger tube **6** (diameter ~9.5 Å), it can be comfortably housed inside the 30-membered cyclobisamide **7** (−CO−(CH$_2$)$_{20}$−CO−Cyst−). An increase in the Ham ratio[13] of the emission spectrum of pyrene, from 0.65 to 0.8 to 1.00 in cyclobisamides **5**, **6**, and **7**, respectively, shows that the polarity monitored by pyrene in nanotube **7** is comparable to that in surfactant micelles.[13b] That the pyrene molecule is completely inside the cavity of **7** was shown by the almost negligible fluorescence quenching of pyrene probe by Cu^{2+} (Figure 9b). Partial quenching in the case of **6** indicates only a small amount of pyrene in the interior of the tube. When in water, or in the presence of **5**, the pyrene emission is totally quenched by Cu^{2+} ions (Figure 9b). Studies on the excimer fluorescence of pyrene (intermolecular excimers formed by the free pyrene as well as intramolecular excimers formed by dipyrenyl molecules such as dipyrenylmethyl ether or DPME[14] and 3,12-bispyrenyl carboxy methyl cholate or BPCM[15]) in the presence of cyclobisamide tubes **6** and **7** showed interesting results. The reduction in the fluorescence intensity of pyrene (I_{500}/I_{390} ratio) from 1.1 and 4.2 (at pyrene concentrations of 12 and 125 μM, respectively, in water) to 0.2 and 1.7 in the presence of **7** (230 μM) indicates that accommodation of two pyrene units within the cavity of **7** causes steric crowding. Similar results were obtained with dipyrenyl probes. Using DPME, the I_{500}/I_{390} ratio of the excimer to monomer band was found to drop from 5.4 in water to 0.62 in **6** and to 0.3 in **7**. Likewise, the ratio for BPCM dropped from 9.5 in water to 2.8 and 2.4 in the presence of **6** and **7**, respectively. For comparison, we found that this ratio for BPCM in the neat organic solvents octanol and hexadecane was 0.5 and 0.7, respectively. This result suggested that the hydrophobic crowding of two pyrene moieties that occurs in water and enhances the excimer emission is absent in organic solvents. In the case of cyclobisamide tubes, the cavity size is apparently not large enough to be able to accom-

(12) Robertson, J. M.; White, J. G. **1947**, 358. (b) Soutar, A. K.; Pownall, H. J.; Hu, S. A. *Biochemistry* **1974**, *13*, 2828.

(13) The ratio of the intensities of the vibronic fine structure bands 3 and 1 in the emission spectrum of pyrene (I_3/I_1) is often called the Ham ratio and is used as an indicator of the polarity of the medium in which pyrene is placed. (a) Nakajima, A. *Bull. Chem. Soc. Jpn.* **1971**, *44*, 3272. (b) Kalyanasundaram, K.; Thomas, J. K. *J. Am. Chem. Soc.* **1977**, *99*, 2039. (c) Dong, D. C.; Winnik, M. A. *Photochem. Photobiol.* **1982**, *35*, 17.

(14) Zachariasse, K. A.; Vaz, W. L. C.; Sotomayor, C.; Kuhnle, W. *Biochim. Biophys. Acta* **1982**, *688*, 323.

(15) Maitra, U.; Rao, P.; Vijay Kumar, P.; Balasubramanian, R.; Mathew, L. *Tetrahedron Lett.* **1998**, *39*, 3255.

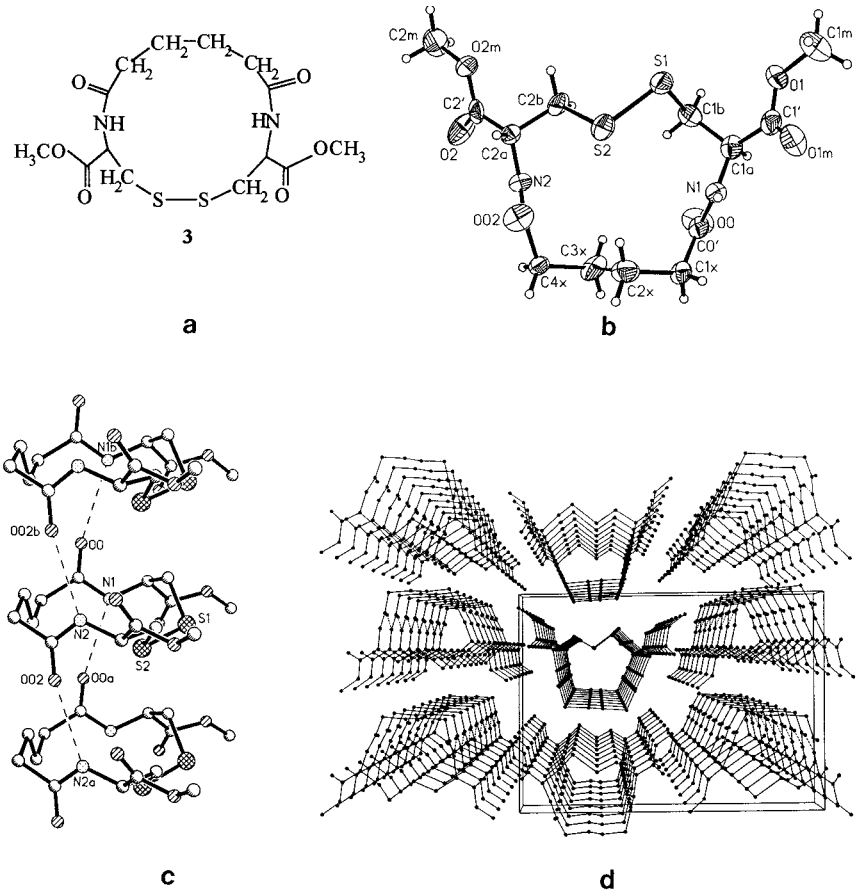

Figure 5. (a) Molecular formula of cyclobisamide **3**. (b) Crystal structure of **3**. Cavity size: 5.50 Å (N2−N1) × 3.95 Å (S2−C2x). Some important bond distances (Å): S1−S2 (2.025), S1−C1b (1.800), S2−C2b (1.818), C1b −C1a (1.541), C2b−C2a (1.546). (c) Hydrogen-bonded vertical stack of **3**. The molecules of **3** aligned in a parallel fashion stack on top of one another and form strings of hydrogen bonds (NH···O═C) on either side of the stack. (d) Side-by-side stacking of cyclobisamide nanotubes. The hollow open-ended tubes are held together in the pack only by hydrophobic forces.

modate two pyrenes. Experiments with perylene gave similar results.

The 30-membered cyclobisamide tube **7** displays a similar interaction with Nile Red, a fluorescent probe dye. As shown in Figure 10, the Nile Red emission blue shifts from 650 nm (in water) to 572 nm in **7**, and increases in intensity by almost 90-fold as compared to that in water. Interestingly, while the lower homologue **5** hardly changes the emission properties, the next higher homologue **6** enhances the emission of Nile Red only by a marginal value and blue shifts from 650 to 615 nm, indicating very little interaction. Nile Red is estimated to have a molecular length of ∼10 Å and width of 7 Å. The fact that its spectral properties are not affected in **5** and marginally so in **6** is consistent with their cavity sizes as determined by X-ray crystallographic studies (vide supra). The cavity of 30-membered cyclobisamide **7** appears to be large enough to accommodate Nile Red and offers it a medium polarity that is low enough to stabilize the nonpolar excited state of the probe from where the radiative path of return to the ground state is preferred over the nonradiative twisted internal charge-transfer (TCIT) mode. The polarity (estimated in terms of the Dimroth scale[16] of $E_T(30)$ values) in the cavity of **7** is estimated at ∼36.6 which compares well with those of solvents dioxane and hexadecane.[17] Interestingly, Nile Red encapsulated in the supercages of the zeolite 13 X of diameter ∼13 Å experiences a polarity value of ∼55.5 (equivalent to 40% dioxane in water). It is possible to raise the alternate possibility that the arenes and Nile Red are not housed in the cavity of the cyclobisamide but are accommodated at the interfacial sites generated when several tubes of **5**, **6**, or **7** self-associate through hydrophobic stacking. We consider this unlikely, since we would expect **5** and **6** to behave similarly to **7** at proportionately higher concentrations. Figure 9a shows that even at concentrations as high as 300 μM **6** and 600 μM **5**, no binding of purene occurs, while it does so readily with 100 μM **7** and levels off beyond this concentration.

Perhaps the most significant result with cyclobisamide tubes was the induction of ordered secondary structure in linear peptides. Melittin, a 26-residue bee-venom peptide with a sequence GIGAVLKVLTTGLPALISWI-KRKRQQNH$_2$, which normally displays a random-coil conformation in water and adopts α-helical structure in a medium of low polarity, e.g., water−organic solvent mixtures or surfactant micelles,[18] was examined for any conformational changes in aqueous medium in the presence of cystine nanotubes. Figure 11 shows that an ordered secondary structure is induced in melittin as the

(16) Dimroth K.; Riechardt, C.; Siepmann, T.; Bohlmann, F. *Liebigs Ann. Chem.* **1963**, *661*, 1.

(17) Sarkar, N.; Das, K.; Bhattacharya, K. *Langmuir* **1994**, *10*, 326.

(18) Chandani, B.; Balasubramanian, D. *Biopolymers* **1986**, *25*, 1259.

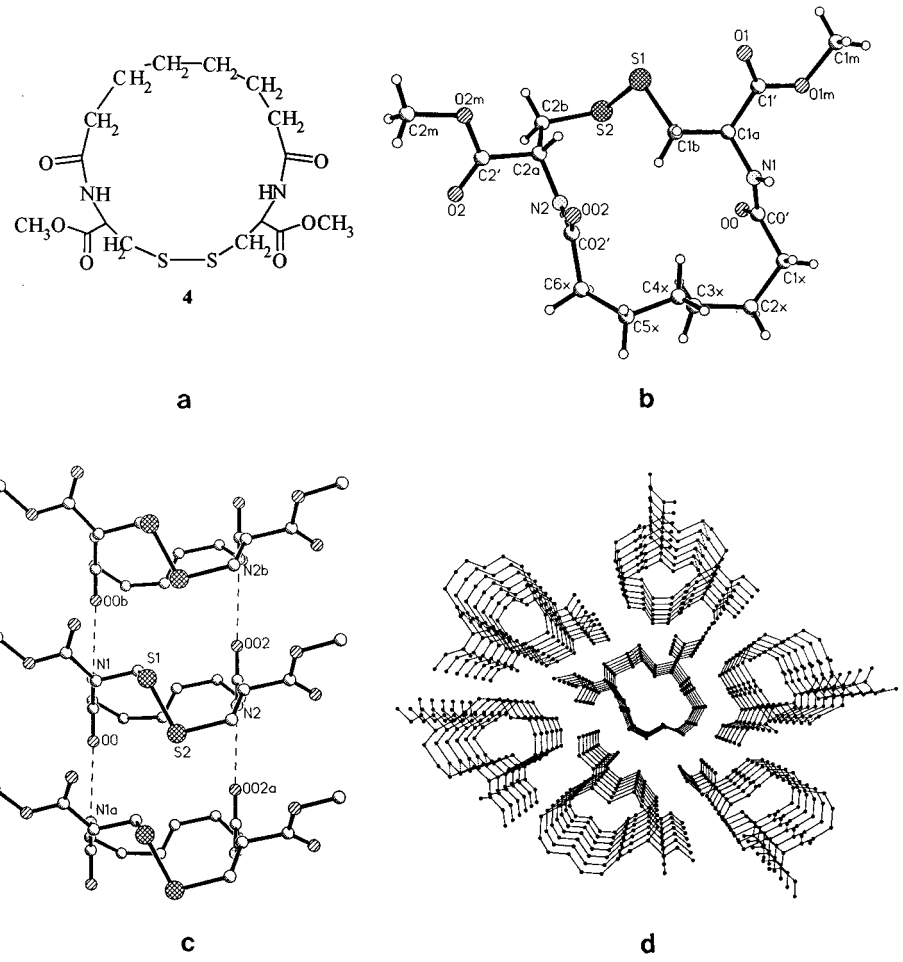

Figure 6. (a) Molecular formula of cyclobisamide **4**. (b) Crystal structure of **4**. Some important bond distances (Å): S1−S2 (2.017), S1−C1b (1.819), S2−C2b (1.819), C1b−C1a (1.525), C2b−C2a (1.522). Cavity size: 5.29 (C02′−C0′) × 4.31 (C1b−C4x) Å. (c) Vertical hydrogen bonding in **4** extending into a tubular structure. The tubes are empty and extend to infinity. (d) Side-by-side packing of nanotubes in **4**.

amount of cyclobisamide **7** is increased. The presence of a negative CD band in the 222−227 nm region is suggestive of the induction of α-helical order. At the highest level of solubility of **7**, namely, 600 μM, the residue molar ellipticity value rises to ∼−11 000, suggesting the induction of about 30% helicity. These results can be interpreted on the basis of one of two models. The first one that we call the "bangle stand", wherein the conformationally ordered melittin is threaded into the cavity of **7** and the complex assembled as a host tube or cylinder containing the melittin. The second is the "Christmas tree" or "hat-stand" model in which each of several nonpolar side chains of melittin are "decorated" or covered by a 30-membered cyclobisamide ring. Interestingly, though, such induction of chain order in melittin was not seen when we used **5** or **6** as the host system. In the absence of further corroborative data, which are unfortunately difficult to obtain in solution because of the limited solubility of the cyclobisamides, we cannot at the moment choose between the models. Cocrystallization of the melittin with **7** and its X-ray diffraction analysis would be of interest.

Conclusion

In summary, the present work introduces a new concept in the design of peptide nanotubes. Simple cyclobisamides prepared in a single step by the condensation of cystine diOMe with 1,ω-alkane dicarbonyl dichloride are shown to form parallel arrays of tubular structures. A crucial structural feature in self-assembling cyclobisamides appears to be the positioning of the two amide groups at almost opposite poles of the ring. The design—essentially closing the polymethylene chain with the cystine diOMe—is flexible with respect to the ring size and permits the creation of a large variety of peptide tubes with adjustable internal diameter, as demonstrated here by the preparation of cyclobisamides with ring size varying from 14- to 20-membered, creating tubes with 5−10 Å internal diameter. The hydrogen-bonded tubes are hollow and open ended and extend to infinity. The hydrophobic interior of the polymethylene-bridged tubes creates a microenvironment suitable for encapsulating lipophilic substances. Fluorescence experiments have shown that the cystine tubules of appropriate diameter enhance the solubility of highly lipophilic arenes, bind to fluorescent probe dyes such as Nile Red, and induce an ordered secondary structure in linear peptides as demonstrated here with 26-residue bee-venom peptide melittin. The general strategy described here should allow the design and synthesis of a wide range of amide-based tubular structures with specified internal diameter and modified surface properties with potential application in inclusion chemistry, catalysis, and drug delivery.

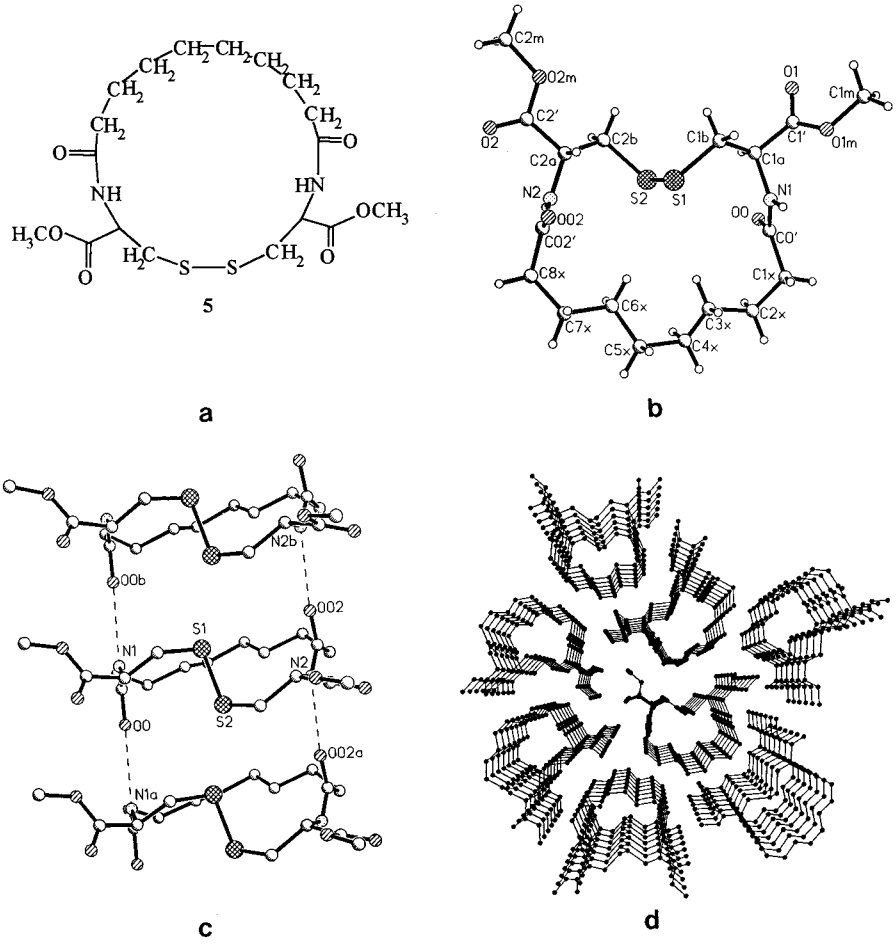

Figure 7. (a) Molecular formula of cyclobisamide **5**. (b) Crystal structure of **5**. Cavity size: 7.06 (C02′−C0′) × 4.39 (S2−C3x) Å. Some important bond distances (Å): S1−S2 (2.031), S1−C1b (1.757), S2−C2b (1.813), C1b−C1a (1.508), C2b−C2a (1.535). (c) Tubular stack in **5**, held together by contiguous NH···O═C hydrogen bonding between the subunits. The hydrogen bond parameters are listed in Table 1. (d) Packing of nanotubes in **5**.

Experimental Section

Melting points are uncorrected. ^{1}H NMR−ROESY experiments were performed using 0.2 and 0.3 s mixing times with pulsed spin locking with 30° pulses and a 2 kHz spin locking field. Reactions were monitored wherever possible by TLC. Silica gel G (Merck) was used for TLC, and column chromatography was done on silica gel (100−200 mesh) columns, which were generally made from a slurry in hexane or a mixture of hexane and ethyl acetate. Products were eluted with a mixture of either ethyl acetate/hexane or chloroform/methanol.

Melittin was obtained from Serva, Germany, and used at a final concentration of 3 μM. The CD spectra were measured in water at ambient pH and temperature, at various concentrations of the cyclic host ranging from 0 to 600 μM.

Crystal Structure Analysis. X-ray data were collected at room temperature on a Bruker automated four-circle diffractometer in the $\theta/2\theta$ mode, with a constant speed of 10 deg/min, 2° scan width, and $2\theta_{max} \approx 115°$ (resolution 0.9 Å), using Cu Kα radiation (λ = 1.541 78 Å), and a graphite monochromator. Structures were determined routinely with direct phase determining procedures. Full matrix, anisotropic least-squares refinement on $|F_o|^2$ was performed on the parameters for all the atoms except the H atoms. The H atoms were placed in idealized positions and allowed to ride with the C or N atom to which each was bonded. All the crystals were in the shape of extremely fine needles with cross-sections of 0.01−0.08 mm.

(**3**) $C_{14}H_{22}N_2O_6S_2$, $P2_12_12$, a = 16.489(1) Å, b = 23.049(1) Å, c = 4.864(1) Å, V = 1848.6 Å^3, d_{calcd} = 1.360 g/cm^3, R1 = 0.0605 for 1132 data with $|F_o| > 4\sigma$, wR2 = 0.1497 for all 1680 data.

(**4**) $C_{16}H_{26}N_2O_6S_2$, $P2_12_12$, a = 19.171(2) Å, b = 21.116(2) Å, c = 5.0045(4) Å, V = 2025.9 Å^3, d_{calcd} = 1.333 g/cm^3, R1 = 0.0417 for 2045 data with $|F_o| > 4\sigma(F)$, wR2 = 0.1187 for all 2169 data. Two-positional disorder for atoms C3x and C3x′ was included in the refinement.

(**5**) $C_{18}H_{30}N_2O_6S_2$, $P2_12_12_1$, a = 5.022(1) Å, b = 17.725(3) Å, c = 25.596(3) Å, V = 2278.4 Å^3, d_{calcd} = 1.267 g/cm^3, R1 = 0.0838 for 931 data with $|F_o| > 4\sigma(F)$, R2 = 0.2425 for all 1702 data. Two-positional disorder for atoms C3x and C3x′ was included in the refinement.

(**6**) $C_{20}H_{34}N_2O_6S_2$, C2, a = 40.698(15) Å, b = 5.083(3) Å, c = 12.105(5) Å, β = 99.66(3)°, V = 2468.6, d_{calcd} = 1.239 g/cm^3, R1 = 0.0859 for 1100 data with $|F_o|^2 > 4\sigma$ and wR2 = 0.1266 for all 1819 data. Distance restraints were applied to atoms C3x to C9x. Two-positional disorder for methyl ester group 2 was included in the refinement.

General Procedure for the Preparation of Macrocyclic Bisamides. a. 1,ω-Alkane dicarboxylic acids were converted into dicarbonyl dichlorides either by refluxing with a 4 M excess of $SOCl_2$ (neat, ~2 h, 80 °C) and evaporating the excess $SOCl_2$ in a vacuum, or by stirring in dry benzene solution with oxalyl chloride (4 M excess containing a few drops of dry pyridine) at room temperature for 24 h, followed by filtration and evaporation of solvents. The residue in both procedures was thoroughly dried and directly used for condensation with cystine diOMe.

b. A solution of freshly prepared 1,ω-alkane dicarbonyl dichloride (2 mmol) in dry CH_2Cl_2 (~100 mL) was added dropwise over 0.5 h to a well-stirred solution of L-cystine dimethyl ester dihydrochloride (2 mmol) and triethylamine (9 mmol) in dry CH_2Cl_2 (~250 mL) at 0 °C. The reaction mixture

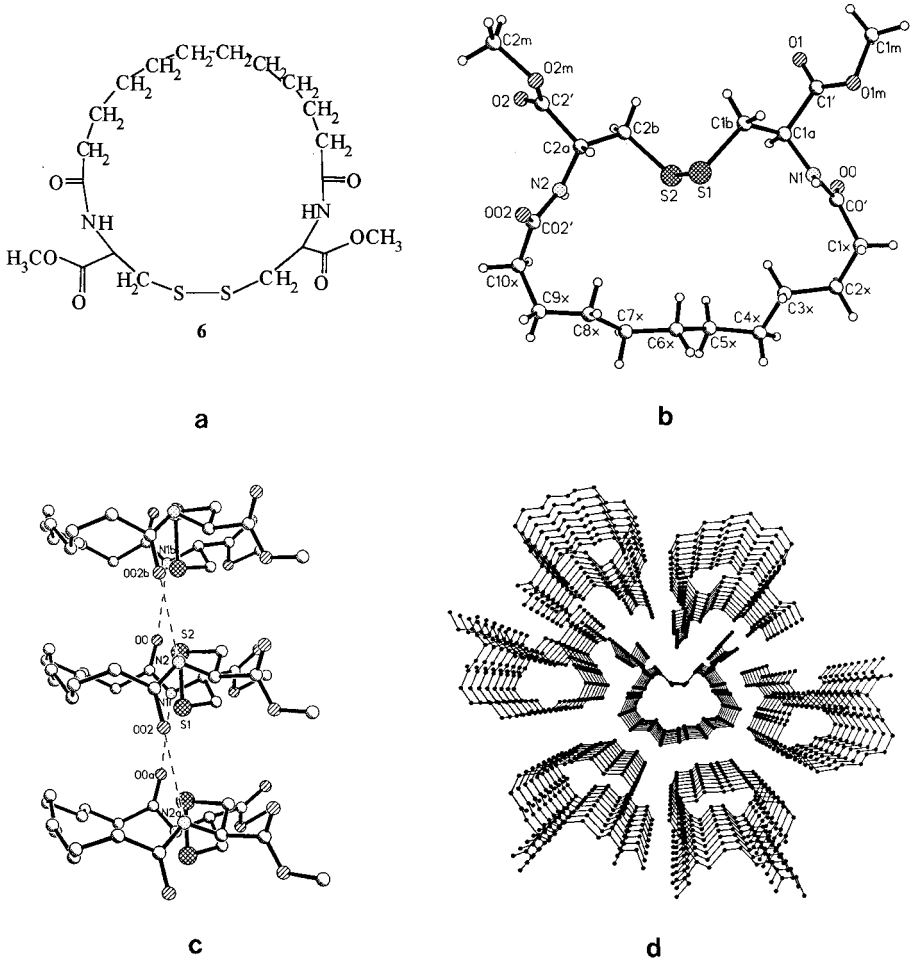

Figure 8. (a) Molecular formula of cyclobisamide **6**. (b) Crystal structure of **6**. Cavity size: 9.49 (C10x−C1x) × 4.52 (S1−C6x) Å. Some important bond distances (Å): S1−S2 (2.018), S1−C1b (1.767), S2−C2b (1.815), C1b−C1a (1.485), C2b−C2a (1.535). (c) Tubular structure in **6** formed by contiguous hydrogen bonding between the subunits. (d) Side-by-side packing of nanotubes in **6**.

was stirred at room temperature for 4−6 h and monitored by TLC. The reaction mixture was washed, sequentially, with ice-cold 2 N H_2SO_4, H_2O, and 5% $NaHCO_3$ (~20 mL each). The organic layer was dried over anhydrous $MgSO_4$ and concentrated in vacuo. The residue was chromatographed on silica gel using either EtOAc/hexane or $CHCl_3$/MeOH for gradient elution. In some cases the precipitated solid in the reaction mixture was separated and the filtrate worked up as above.

Selected Data. Cyclo(Succ−Cyst): yield 11.8%; mp 230−231 °C; IR (KBr) 3332, 3307, 1747, 1649, 1538 cm^{-1}; ^1H NMR (300 MHz, $CDCl_3$) δ 2.28 (2H, m), 2.55 (4H, m), 2.88 (2H, m), 3.65 (6H, s), 4.64 (2H, m), 8.21 (2H, br d); FAB MS *m*/*z* (rel intens): 351 (100) $(MH)^+$.

Cyclo(Succ−Cyst)$_2$: yield 9.1%; mp 243−244 °C; IR (KBr) 3473, 3325, 1745, 1649, 1555 (sh), 1533 cm^{-1}; ^1H NMR (300 MHz, $CDCl_3$) δ 2.33 (8H, m), 2.75 (4H, m), 3.01 (4H, m), 3.64 (12H, s), 4.61 (4H, m), 8.52 (4H, d, J = 7.85 Hz); FAB MS *m*/*z* (rel intens): 701 (100) $(MH)^+$.

Cyclo(Glut−Cyst): yield 9.3%; mp 224−226 °C; $[\alpha]^{29}_D$ −149.84 (*c* 2.3, $CHCl_3$/MeOH, 3:1); IR (KBr) 3348, 3316, 2945, 1737, 1650, 1547 cm^{-1}; ^1H NMR (300 MHz, DMSO-d_6) δ 1.79 (2H, m), 2.21 (4H, m), 2.90 (2H, m), 3.33 (2H, m), 3.63 (6H, m), 4.72 (2H, m), 8.29 (2H, d, J = 9 Hz); FAB MS *m*/*z* (rel intens) 365 (100) $(MH)^+$.

Cyclo(Glut−Cyst)$_2$: yield 20.3%; mp 200−203 °C; $[\alpha]^{29}_D$ −115 (*c* 2.3, $CHCl_3$/MeOH, 3:1); IR (KBr) 3331, 2960, 1743, 1652, 1542 cm^{-1}; ^1H NMR (300 MHz, DMSO-d_6) δ 1.70 (4H, m), 2.13 (8H, m), 2.84 (4H, m), 3.07 (4H, m), 3.63 (12H, s), 4.54 (4H, m), 8.31 (4H, d, J = 8 Hz); FAB MS *m*/*z* (rel intens) 729 (100) $(MH)^+$.

Cyclo(Glut−Cyst)$_3$: yield 5.4%; mp 198−200 °C; $[\alpha]^{29}_D$ −56.039 (*c* 0.46, $CHCl_3$/MeOH, 3:1); IR (KBr) 3319, 2958, 1748, 1655, 1538 cm^{-1}; ^1H NMR (300 MHz, $CDCl_3$) δ 1.69 (6H, m), 2.13 (12H, m), 2.89 (6H, m), 3.09 (6H, m), 3.63 (18H, m), 4.54 (6H, m), 8.34 (6H, d, J = 7.8 Hz); FAB MS *m*/*z* (rel intens) 1093 (100) $(MH)^+$.

Cyclo(Glut−Cyst)$_4$: yield 1.5%; mp 172−174 °C; IR (KBr) 3325, 2960, 1744, 1653, 1533, cm^{-1}; ^1H NMR (300 MHz, DMSO-d_6) δ 1.71 (8H, m), 2.13 (16H, m), 2.91 (8H, m), 3.09 (8H, m), 3.63 (24H, m), 4.53 (8H, m), 8.35 (8H, d, J = 7.8 Hz).

Cyclo(Glut−Cyst)$_5$: yield 0.3%; IR (KBr) 3333, 2932, 1749, 1658, 1537, 1451, 1338, 1223, 1169, 1103 cm^{-1}; ^1H NMR (300 MHz, DMSO-d_6) δ 1.71 (10H, m), 2.14 (20H, m), 2.92 (10H, m), 3.11 (10H, m), 3.64 (10H, s), 4.54 (10H, m), 8.36 (10H, d, J = 7.8 Hz); FAB MS *m*/*z* (rel intens) 1821 (100) $(MH)^+$.

Cyclo(Glut−Cyst)$_6$: yield 0.2%; ^1H NMR (300 MHz, DMSO-d_6) δ 1.67 (12H, m), 2.11 (24H, m), 2.93 (12H, m), 3.09 (12H, m), 3.62 (36H, m), 4.53 (12H, m), 8.36 (12H, d, J = 7.8 Hz); FAB MS *m*/*z* (rel intens) 2186 (35) $(MH)^+$.

Cyclo(Adip−Cyst): yield 20.4%; mp 223−224 °C; IR (KBr) 3316, 3062, 2964, 2941, 2873, 1752, 1647, 1542 cm^{-1}; ^1H NMR (300 MHz, $CDCl_3$) δ 1.55 (4H, m), 2.37 (4H, m), 3.19 (2H, m), 3.78 (6H, s), 4.97 (2H, m), 6.58 (2H, d, J = 6.32 Hz); FAB MS *m*/*z* (rel intens) 379 (100) $(MH)^+$.

Cyclo(Adip−Cyst)$_2$: yield 1.2%; ^1H NMR (300 MHz, $CDCl_3$) δ 1.47 (8H, br s), 2.11 (8H, br s), 2.84 (4H, m), 3.05 (4H, m), 3.65 (12H, s), 4.57 (4H, m), 8.35 (4H, br d); FAB MS *m*/*z* (rel intens) 757 (45) $(MH)^+$.

Cyclo(Adip−Cyst)$_3$: yield 1.0%; ^1H NMR (300 MHz, $CDCl_3$) δ 1.50 (2H, br s), 2.14 (12H, br s), 2.93 (2H, m), 3.13 (2H, m), 3.65 (18H, s), 4.57 (6H, m), 8.33 (6H, br d); FAB MS *m*/*z* (rel intens) 1135 (34) $(MH)^+$, 1267 (100) $(M + Cs^+)$.

Cyclo(Pim−Cyst): yield 10.5%; mp 225−226 °C; IR (KBr) 3322, 3277, 3082, 2963, 2929, 2861, 1741, 1651, 1552 cm^{-1};

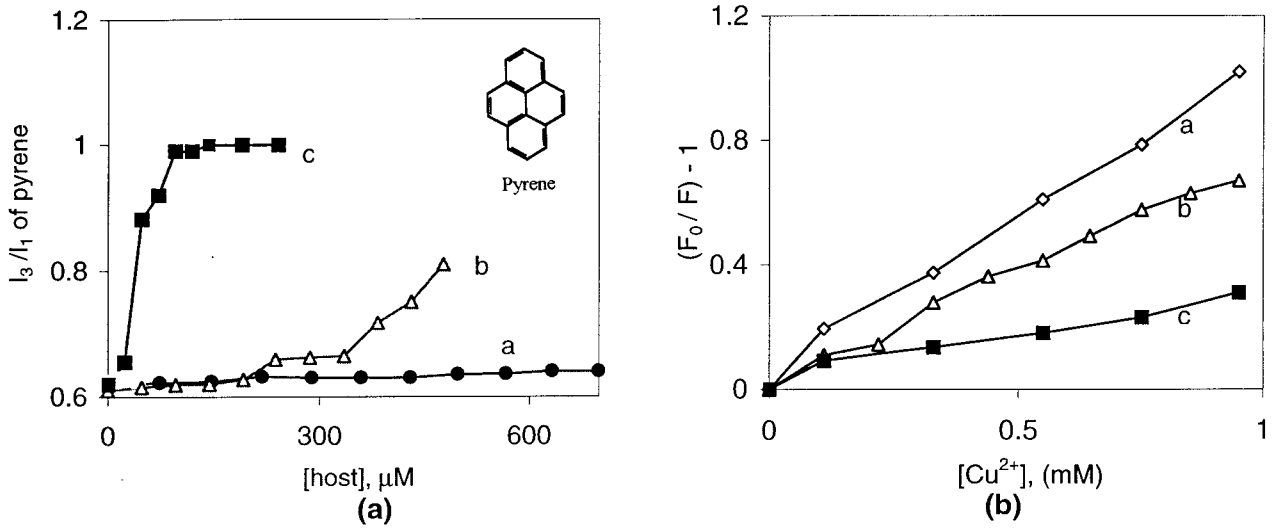

Figure 9. Sequestration of pyrene in the host systems: Panel a shows variation of the Ham ratio (I_3/I_1) of pyrene in the presence of increasing amounts of (a) **5**, (b) **6**, and (c) **7**. Panel b shows the Stern−Volmer quenching of the emission of aqueous Cu^{2+}. The key is the same as in panel a.

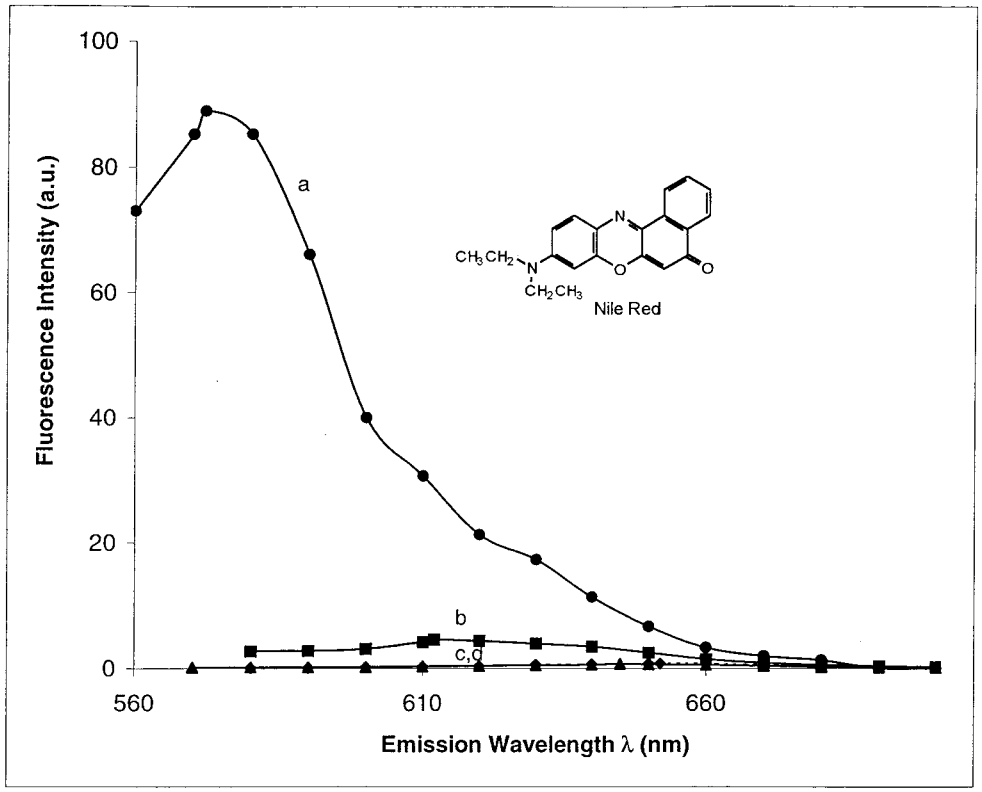

Figure 10. Polarity sensing by Nile Red: emission spectra of Nile Red (2 μM) in aqueous solutions of cyclobisamides (a) **7**, (b) **6**, (c) **5**, and (d) 5% v/v MeOH. The band maximum wavelength of the dye in the solution of **7** is the same as in neat dioxane or hexadecane, though the intensity is higher.

^{1}H NMR (300 MHz, DMSO-d_6) δ 1.15 (2H, m), 1.39 (2H, m), 1.58 (2H, m), 2.09 (4H, m), 2.77 (2H, m), 3.14 (2H, m), 3.63 (6H, s), 4.57 (2H, m), 8.50 (2H, d, J = 8.10 Hz); FAB MS m/z (rel intens) 393 (56) $(MH)^+$.

Cyclo(Pim−Cyst)$_2$: yield 3.0%; mp 206−207 °C; IR (KBr) 3324, 3082, 2951, 2872, 1746, 1652, 1557 (sh), 1534 cm^{-1}; ^{1}H NMR (300 MHz, DMSO-d_6) δ 1.24 (4H, m), 1.47 (8H, m), 2.06 (8H, m), 2.83 (4H, m), 3.07 (4H, m), 3.63 (12H, s), 4.55 (4H, m), 8.33 (4H, d, J = 7.8 Hz); FAB MS m/z (rel intens) 785 (100) $(MH)^+$.

Cyclo(Pim−Cyst)$_3$: yield 2%; mp 180−181 °C; IR (KBr) 3324, 3069, 2954, 2866, 1747, 1544, 1532 (sh) cm^{-1}; ^{1}H NMR (300 MHz, DMSO-d_6) δ 1.23 (6H, m), 1.47 (12H, m), 2.09 (12H, m), 2.89 (6H, m), 3.09 (6H, m), 3.63 (s, 18H), 4.54 (6H, m), 8.33 (6H, d, J = 7.8 Hz); FAB MS m/z (rel intens) 1177 (100) $(MH)^+$, 785 (22) (M − (Pim−Cyst) + H)$^+$, 393 (M − 2(Pim−Cyst) + H)$^+$.

Cyclo(Pim−Cyst)$_4$: yield 1.1%; ^{1}H NMR (300 MHz, DMSO-d_6) δ 1.23 (8H, m), 1.47 (16H, m), 2.09 (16H, m), 2.90 (8H, m), 3.10 (8H, m), 3.63 (24H, m), 4.53 (8H, m), 8.33 (8H, d, J = 7.8 Hz); FAB MS m/z (rel intens) 1569 (100) $(MH)^+$, 1177 (27) (M − (Pim−Cyst) + H)$^+$, 785 (31) (M − 2(Pim−Cyst) + H)$^+$, 393 (7) (M − 3(Pim−Cyst) + H)$^+$.

Cyclo(Sub−Cyst): yield 30.0%; mp 207−208 °C; IR (KBr) 3339, 3289, 3081, 2943, 2863, 1744, 1655, 1536 cm^{-1}; ^{1}H NMR (300 MHz, DMSO-d_6) δ 1.13 (4H, m), 1.38 (2H, m), 1.65 (2H,

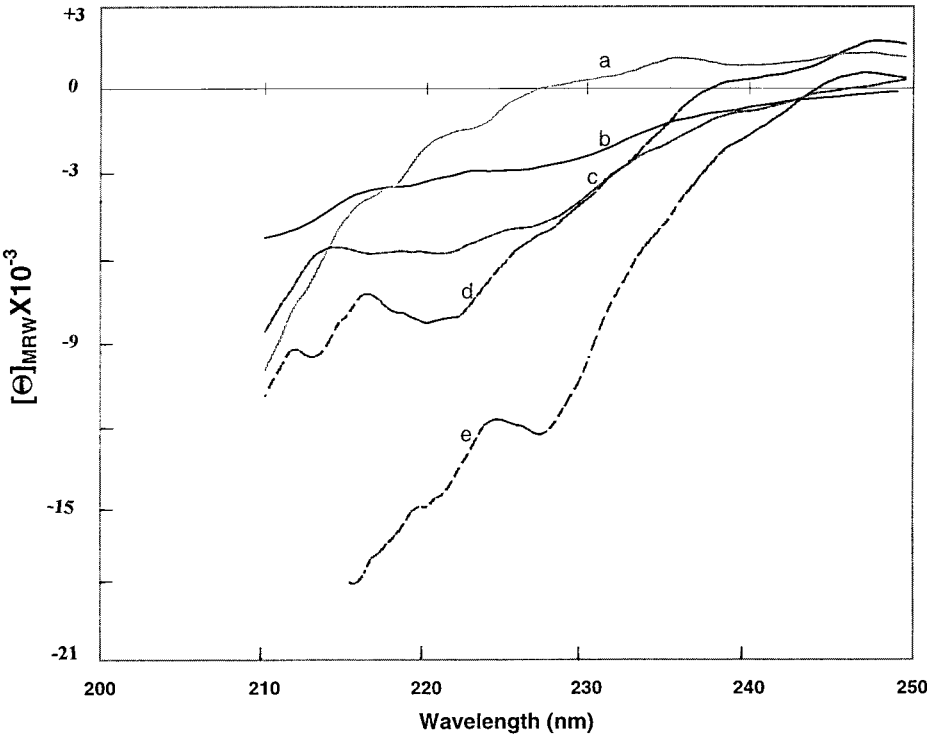

Figure 11. Induction of helical order in melittin: residue molar ellipticity of melittin (3.3 μM) in aqueous solutions of **7**, with increasing concentrations of (a) 0, (b) 91, (c) 214, (d) 400, and (e) 569 μM, respectively.

m), 2.07 (4H, m), 2.65 (2H, m), 3.09 (2H, m), 3.62 (6H, s), 4.57 (2H, m), 8.44 (2H, d, J = 8.1 Hz); FAB MS m/z (rel intens) 407 (100) $(MH)^+$.

Cyclo(Sub−Cyst)$_2$: yield 16.0%; mp 213−214 °C; IR (KBr) 3334, 3049, 2945, 2864, 1755, 1657, 1561, 1530 cm^{-1}; ^{1}H NMR (300 MHz, DMSO-d_6) δ 1.22 (8H, m), 1.45 (8H, m), 2.08 (8H, m), 2.85 (2H, m), 3.07 (2H, m), 3.62 (12H, s), 4.55 (4H, m), 8.33 (4H, d, J = 7.8 Hz); FAB MS m/z (rel intens) 813 (100) $(MH)^+$.

Cyclo(Sub−Cyst)$_3$: yield 5.0%; mp 172−173 °C; IR (KBr) 3332, 3046, 2943, 2863, 1748, 1655, 1534 cm^{-1}; ^{1}H NMR (300 MHz, DMSO-d_6) δ 1.22 (12H, m), 1.46 (12H, m), 2.09 (12H, m), 2.89 (6H, m), 3.09 (6H, m), 3.63 (18H, s), 4.55 (6H, m), 8.32 (6H, d, J = 7.8 Hz); FAB MS m/z (rel intens) 1219 (100) $(MH)^+$.

Cyclo(Seb−Cyst): yield 31.0%; mp 203−204 °C; ^{1}H NMR (300 MHz, DMSO-d_6) δ 0.93−1.68 (12H, m), 2.10 (4H, br s), 2.67 (2H, m), 3.13 (2H, m), 3.64 (6H, s), 4.72 (2H, m), 8.26 (2H, d, J = 8.4 Hz); FAB MS m/z (rel intens) 435 (100) $(MH)^+$.

Cyclo(Seb−Cyst)$_2$: yield 15.0%; mp 211−213 °C; IR (KBr) 3330, 3038, 2934, 2859, 1752, 1656, 1533 cm^{-1}; ^{1}H NMR (300 MHz, DMSO-d_6) δ 1.21 (16H, brs), 1.46 (8H, m), 2.08 (8H, m), 2.85 (4H, m), 3.07 (4H, m), 3.62 (12H, s), 4.55 (4H, m), 8.33 (4H, d, J = 7.8 Hz); FAB MS m/z (rel intens) 868 (100) $(MH)^+$.

Cyclo(Dodeca−Cyst): yield 29.0%; mp 228−230 °C; IR (KBr) 3335, 3059, 2935, 2861, 1742, 1654, 1557, 125, 1534 cm^{-1}; ^{1}H NMR (300 MHz, $CDCl_3$) δ 1.26 (12H, br s), 1.52 (2H, br s), 1.69 (2H, br s), 2.23 (4H, br s), 2.90 (2H, m), 3.15 (2H, m), 3.73 (6H, s), 4.84 (2H, m), 7.81 (2H, d, J = 5.85 Hz); FAB MS m/z (rel intens) 463 (100).

Cyclo(Docosane−Cyst): yield 20.0%; mp 162−163 °C; IR (KBr) 3331, 3077, 2933, 2861, 1744, 1654, 1551, 1534 cm^{-1}; ^{1}H NMR (300 MHz, $CDCl_3$) δ 1.28 (34H, br s), 1.67 (6H, m), 2.25 (4H, m), 3.20 (4H, m), 3.78 (6H, s), 4.87 (2H, m), 6.48 (2H, d, J = 7.5 Hz); ^{13}C NMR (75 MHz, $CDCl_3$) 173.23, 171.01, 52.74, 51.58, 40.64, 36.46, 29.07, 28.40, 28.35, 25.49; FAB MS m/z (rel intens) 603 (100) $(MH)^+$.

Acknowledgment. We are grateful to Dr. Klaas Zachariasse of the Max Planck Institute for Biophysical Chemists, Göttingen, and Professor Uday Maitra of the Indian Institute of Science, Bangalore, for their kind gifts of dipyrenylmethyl ether and 3,12-bispyrenylcholic acid methyl ester, respectively. Financial support from DST, New Delhi, and from the Office of Naval Research and the National Institutes of Health (Grant GM-30902) is acknowledged. D.R. is an honorary faculty member of Jawaharlal Nehru Centre for Advanced Scientific Research.

Supporting Information Available: ^{1}H NMR spectra of cyclo(Succ−Cyst), cyclo(Succ−Cyst)$_2$, cyclo(Adip−Cyst), cyclo(Adip−Cyst)$_2$, cyclo(Adip−Cyst)$_3$, cyclo(Pim−Cyst), cyclo(Pim−Cyst)$_2$, cyclo(Pim−Cyst)$_3$, cyclo(Pim−Cyst)$_4$, cyclo(Sub−Cyst), cyclo(Sub−Cyst)$_2$, cyclo(Sub−Cyst)$_3$, cyclo(Seb−Cyst), cyclo(Seb−Cyst)$_2$, cyclo(dodec−Cyst), and cyclo(Docosane−Cyst); ROESY spectrum of cyclo(Glut−Cyst); ^{13}C NMR spectrum of cyclo(Dodec−Cyst); FAB MS of cyclo(Succ−Cyst), cyclo(Succ−Cyst)$_2$; combined FAB MS of cyclo(Adip−Cyst), cyclo(Adip−Cyst)$_2$, and cyclo(Adip−Cyst)$_3$; combined FAB MS of cyclo(Pim−Cyst), cyclo(Pim−Cyst)$_2$, cyclo(Pim−Cyst)$_3$, and cyclo(Pim−Cyst)$_4$; combined FAB MS of cyclo(Sub−Cyst), cyclo(Sub−Cyst)$_2$, and cyclo(Sub−Cyst)$_3$ with combined FAB MS of cyclo(Seb−Cyst), cyclo(Seb−Cyst)$_2$, and cyclo(Docosane−Cyst); and X-ray diffraction information for **3**−**6** including data collection and refinement information, coordinates, bond lengths and angles, anisotropic thermal parameters, and coordinates for hydrogen atoms. This material is available free of charge via the Internet at http://pubs.acs.org.

JO991378M